

Interface ordering and phase competition in a model Mott-insulator-band-insulator heterostructure

Satoshi Okamoto* and Andrew J. Millis

Department of Physics, Columbia University, 538 West 120th Street, New York, New York 10027, USA

(Received 7 June 2005; revised manuscript received 29 August 2005; published 7 December 2005)

The phase diagram of model Mott-insulator-band-insulator heterostructures is studied using the semiclassical approximation to the dynamical-mean-field method as a function of thickness, coupling constant, and charge confinement. An interface-stabilized ferromagnetic phase is found, allowing the study of its competition and possible coexistence with the antiferromagnetic order characteristic of the bulk Mott insulator.

DOI: [10.1103/PhysRevB.72.235108](https://doi.org/10.1103/PhysRevB.72.235108)

PACS number(s): 73.20.-r, 71.27.+a, 75.70.-i

The fabrication and investigation of heterostructures involving correlated-electron materials^{1,2} is an important direction in material science. Understanding the electronic properties near the interfaces and surfaces is not only of scientific interest but is also essential to the creation of electronic devices exploiting the unique properties of correlated-electron materials. A variety of heterostructures have been fabricated and studied including high- T_c cuprates,^{3,4} Mott-insulator and band-insulator heterostructure,⁵ and superlattices of transition-metal oxides.⁶⁻⁸ Interestingly, the heterostructures comprised of a Mott insulator and a band insulator were reported to show metallic behavior.⁵

A fundamental question raised by those studies is “what electronic phases are realized at interfaces.” For the vacuum-bulk interface (i.e., the surface), Potthoff and Nolting,⁹ Schwieger, Potthoff, and Nolting,¹⁰ and Liebsch¹¹ have argued that the reduced coordination may enhance correlation effects. The enhanced correlations could presumably induce surface magnetic ordering, although this possibility was not discussed in Refs. 9–11. Matzdorf *et al.* proposed that ferromagnetic ordering is stabilized at the surface of two-dimensional ruthenates by a lattice distortion,¹² but this is not yet observed. Surface ferromagnetism had been also discussed in a mean field treatment of the Hubbard model by Potthoff and Nolting.¹³ Similarly, the effect of bulk strain on the magnetic ordering in perovskite manganites was discussed by Fang, Solovyev, and Terakura.¹⁴

All these studies dealt with systems in which charge densities remain unchanged from the bulk values, and physics arising from the modulation of charge density was not addressed. A crucial aspect of the recently fabricated heterostructures is charge inhomogeneity, caused by the spreading of electrons from one region to another. Strongly correlated materials typically possess interesting density-dependent phase diagrams, raising the possibility of interesting phase behavior at interfaces. In this paper we use the semiclassical approximation (SCA)¹⁵ to the dynamical-mean-field method¹⁶ to explore the phase behavior of a model Mott-insulator-band-insulator heterostructure. The SCA is computationally inexpensive and a good representation of phase diagrams and transition temperatures in several models, allowing us to investigate the phase behavior for a wide range of parameters, and in particular to access the $T > 0$ regime which Hartree-Fock and related approximations fail to rep-

resent adequately.¹⁷ We observe antiferromagnetic ordering in regions with charge density ~ 1 characteristic of a bulk Mott insulator, while ferromagnetic ordering is found to be a surface effect supported by an intermediate charge density and a strong coupling. However, we have found that, despite the successes noted in previous work, the SCA overestimates ferromagnetism on the lattice we study here. Therefore, our results should be regarded as qualitative explanations of the type of phase behavior which may occur rather than as quantitative statements about the Hubbard-model phase diagram.

We study the model heterostructure introduced in Ref. 18. The Hamiltonian is a simplified representation of conduction bands of the systems studied in Ref. 5 with the orbital degeneracy neglected. We consider [001] heterostructures formed by varying the A site of a ABO_3 perovskite lattice. The electrons of interest reside on the B -site ions, which form a simple cubic lattice with sites labeled by i as $\vec{r}_i = a(n_i, m_i, l_i)$ with the lattice constant a set to unity. We assume each B site has a single orbital; electrons hop between nearest neighbor sites with the transfer t . The electrons interact via an on-site interaction U and a long-ranged Coulomb repulsion. The heterostructure is defined by n planes of charge +1 counterions placed on the A' sublattice of A site ions at positions $\vec{r}_j^{A'} = a(n_j + 1/2, m_j + 1/2, l_j + 1/2)$, with $-\infty < n_j, m_j < \infty$ and $l_j = 1, \dots, n$. We present results in terms of a coordinate $z = l_i - n/2$ shifted such that the center of the heterostructure, A' sublattice, comes to $z = 0$. Charge neutrality requires that the areal density of electrons is n . The resulting Hamiltonian is $H = H_{band} + H_{int} + H_{Coul}$ with

$$H_{band} = -t \sum_{\langle ij \rangle, \sigma} (d_{i\sigma}^\dagger d_{j\sigma} + H.c.), \quad (1)$$

$$H_{int} = U \sum_i n_{i\uparrow} n_{i\downarrow} + \frac{1}{2} \sum_{\substack{i \neq j \\ \sigma, \sigma'}} \frac{e^2 n_{i\sigma} n_{j\sigma'}}{\varepsilon |\vec{r}_i - \vec{r}_j|}, \quad (2)$$

$$H_{Coul} = - \sum_{i,j,\sigma} \frac{e^2 n_{i\sigma}}{\varepsilon |\vec{r}_i - \vec{r}_j^{A'}|}. \quad (3)$$

Note that $U \neq 0$ on all sites. A dimensionless measure of the strength of the long-ranged Coulomb interaction is $E_c = e^2 / (\varepsilon at)$ with the dielectric constant ε . In most of our

analysis, we choose $E_c=0.8$. This corresponds to $t\sim 0.3$ eV, $a\sim 4$ Å, and $\varepsilon=15$, which describe the system studied in Ref. 5. The charge profile is found not to depend in an important way on ε , but the stability of magnetic orderings does because this is sensitive to the details of the charge density distribution as discussed later.

The basic object of our study is the electron Green's function. In general, this is given by

$$G_\sigma(\vec{r}, \vec{r}'; \omega) = [\omega + \mu - H_{band} - H_{Coul} - \Sigma_\sigma(\vec{r}, \vec{r}'; \omega)]^{-1}, \quad (4)$$

with the chemical potential μ and the electron self-energy Σ . We consider [001] heterostructures with either in-plane translational invariance or N_s -sublattice antiferromagnetism. The Green's function and self-energy are therefore functions of the variables $(z, \eta, z', \eta', \vec{k}_\parallel)$ where η and $\eta' (=1, \dots, N_s)$ label the sublattice in layers z and z' , respectively, and \vec{k}_\parallel is a momentum in the (reduced) Brillouin zone. As in Ref. 18, we approximate the self-energy as the sum of a static Hartree term Σ_σ^H arising from the long-ranged part of the Coulomb interaction and a dynamical part $\Sigma_\sigma^D(\omega)$ arising from local fluctuations. Generalizing the inhomogeneous case of the dynamical-mean-field theory (DMFT),¹⁰ we assume that the self-energy is only dependent on layer coordinate z and sublattice index η . Thus, the dynamical part of the self-energy is written as

$$\Sigma_\sigma^D \Rightarrow \Sigma_\sigma^D(z, \eta; \omega). \quad (5)$$

The $z\eta$ -dependent self-energy is determined from the solution of a quantum impurity model¹⁶ with the mean-field function fixed by the self-consistency condition

$$G_\sigma^{imp}(z, \eta; \omega) = N_s \int \frac{d^2 k_\parallel}{(2\pi)^2} G_\sigma(z, \eta, z, \eta, \vec{k}_\parallel; \omega). \quad (6)$$

We shall use the DMFT, which is a mean-field approximation, to calculate magnetic phase diagrams of effectively two-dimensional systems, so some mention of fluctuation effects is needed. In general, the calculated transition temperatures are to be understood as crossover scales below which the magnetic correlation length ξ grows rapidly $\xi \sim \exp(2\pi\rho_s/T)$ with spin stiffness ρ_s ¹⁹ which we estimate below. True long-ranged order may be induced at $T>0$ by an Ising anisotropy or by three-dimensional coupling in a system made of repeated heterostructure units. In any event, the rapid growth of the correlations for $T<\rho_s$ means that the properties are effectively those of an ordered state. We will find that the low- T ρ_s is sufficiently large relative to the calculated transition temperature that fluctuation effects are not crucial.

In general, for the heterostructure with L layers with N_s sublattices, one must solve $L \times N_s$ independent impurity models. Due to the self-consistency condition [cf. Eq. (6)] and to compute the charge density $n_\sigma(z, \eta) = -\int d\omega / \pi f(\omega) \text{Im} G_\sigma^{imp}(z, \eta; \omega)$ with f the Fermi distribution function, it is required to invert the $(L \times N_s)^2$ Green's function matrix at each momentum and frequency. This time consuming numerics restrict the size of the unit cell. In this

study, we consider commensurate magnetic states with up to two sublattices, $N_s=1$ and 2, i.e., paramagnetic (PM), ferromagnetic (FM) states, and antiferromagnetic (AF) and layer-AF states where AF and FM planes with moment alternating from plane to plane, respectively. Note that the AF state extrapolates to the bulk AF state with the magnetic vector $\vec{q}=(\pi, \pi, \pi)$ at $n \rightarrow \infty$. By symmetry, the number of quantum impurity models one must solve is reduced to L . However, solution of the impurity models is a time consuming task, and an inexpensive solver is required. In Ref. 18, to study the evolution of the low-energy quasiparticle band and high-energy Hubbard bands as a function of position, we applied two-site DMFT²⁰ which is a simplified version of exact-diagonalization method. At $T=0$, this method is known to give reasonable results for Mott metal-insulator and magnetic transitions. However, the small number of bath orbitals used in the two-site method is known to be insufficient to describe the thermodynamics correctly.¹⁵

For the investigations presented here, we use the semiclassical approximation introduced in Ref. 15. We represent the Hubbard interaction $Un_\uparrow n_\downarrow$ in terms of the total on-site charge n_{tot} and magnetization m as $(1/4)U(n_{tot}^2 - m^2)$, decouple the interaction via auxiliary fields ξ coupling to charge and φ coupling to magnetization. The semiclassical approximation retains only the zero Matsubara frequency (classical) component of φ , but performs the integral over this component exactly, and for each value of φ replaces ξ by the value which minimizes the action at the given value of φ . (For technical details see Ref. 15). The method provides a good representation of the local moment formation and associated slow spin fluctuations characteristic of strongly correlated systems. This method is computationally inexpensive and has been found to be reasonably accurate for phase boundaries and excitation spectra of several models, including the half-filled Hubbard model and, at all fillings, for the $d=3$ and $d=\infty$ face-centered-cubic (fcc) lattices.¹⁵ We note, however, that, perhaps because it does not properly include quasiparticle coherence, the method overemphasizes ferromagnetism at intermediate density, giving for fcc lattices transition temperatures $\sim 50\%$ higher than those found by quantum Monte Carlo,¹⁵ and for cubic lattices, finding ferromagnetism at $n_{tot}=0.5$ and moderately large U (of order the critical value for the Mott transition) when other methods²¹ suggest ferromagnetism is confined to very large U (about six times larger than the Mott critical value) and n_{tot} near 1. Thus, the application of the SCA to Hubbard heterostructure allows a convenient exploration of the interplay between different phases, but probably does not provide a quantitatively reliable picture of the phase diagram of this model.

First, we investigate the magnetic behavior at finite temperature. The upper panel of Fig. 1 shows our calculated phase diagram in the interaction-temperature plane for heterostructures with various thicknesses for charge binding parameter $E_c=0.8$. The one-layer heterostructure is PM at weak to moderate interactions, and FM at strong interactions. The two- and three-layer heterostructures are AF at weak to intermediate interaction, and become FM at stronger interactions with almost the same T_C for $n=2$ and 3. Hartree-Fock studies of this and related models find a layer-AF phase. This phase is not found in our DMFT analysis. Antiferromagnetic

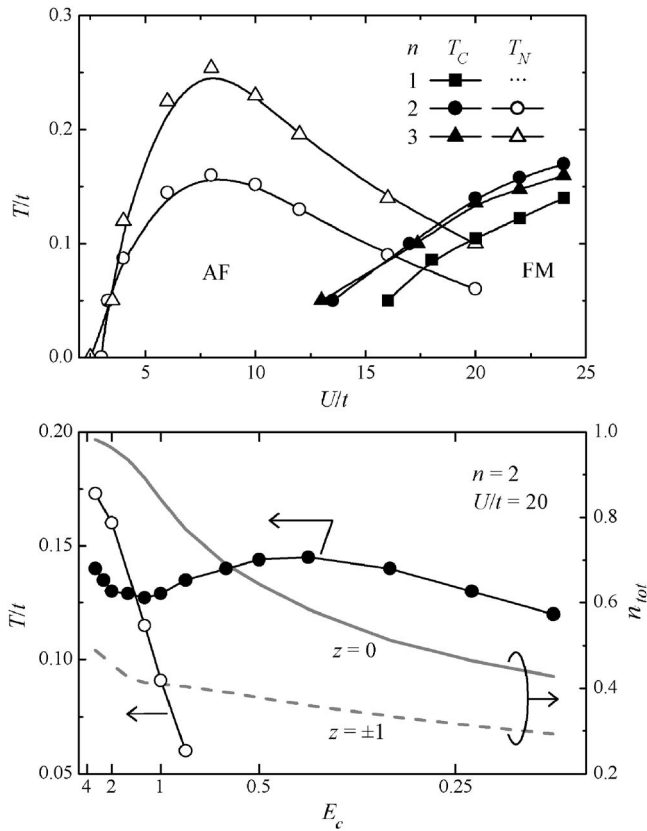


FIG. 1. Upper panel: Magnetic transition temperatures of heterostructures with various thicknesses n indicated as functions of interaction strength. $E_c=0.8$. Filled symbols: Ferromagnetic Curie temperature T_C , open symbols: Antiferromagnetic Néel temperature T_N . Note that, where both phases are locally stable, the phase with higher $T_C(T_N)$ has the lower free energy. Lower panel: Magnetic transition temperatures and charge density n_{tot} at $z=0$ (light solid line) and ± 1 (light broken line) at $T/t=0.1$ as functions of the parameter E_c for two-layer heterostructure with $U/t=20$. Counterions are placed at $z=\pm 0.5$.

Néel temperature T_N is found to increase strongly with the increase of layer thickness. However, these T_N 's are substantially reduced from the bulk values; maximum value $T_N^{max}/t \sim 0.47$ at $U/t \sim 10$, whereas Curie temperature T_C 's are almost the bulk $2d$ values at $n_{tot} \sim 0.5$. The strong dependence of T_N on thickness may be understood from the bulk phase diagram; antiferromagnetism is stabilized only very near to half filling, and in the thinner heterostructures the charge-spreading effect reduces the density too much. This physics is seen from a different point of view in the lower panel of Fig. 1.

The lower panel of Fig. 1 presents a detailed study of the $n=2$ heterostructure showing how changes in the charge confinement parameter E_c affect the physics. The filled and open points (left-hand axis) show the variation of the Curie and Néel temperatures, respectively. The light solid and light broken lines (right-hand axis) show the variation of charge density on the central and next to central layers, respectively. It is seen that the AF ordering is rapidly destabilized with the decrease of E_c (and concomitant decrease of central-layer charge density). On the contrary, T_C has a weak variation

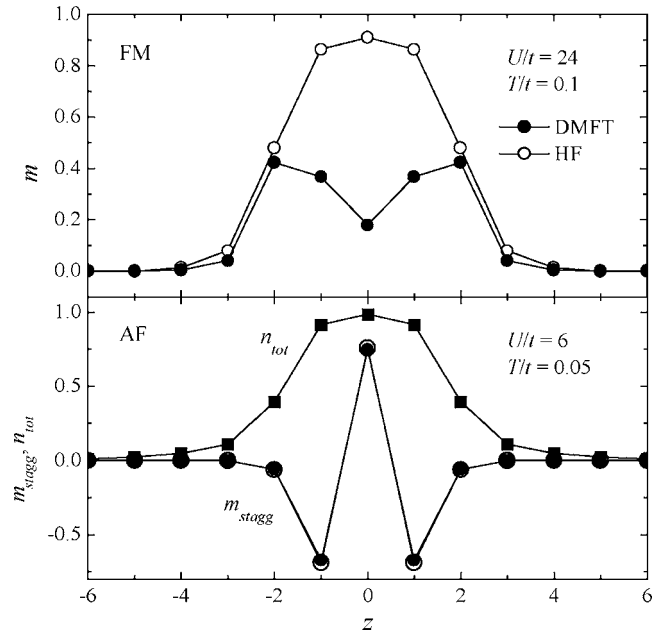


FIG. 2. Magnetization density of four-layer heterostructure. Counterions are placed at $z=\pm 0.5, \pm 1.5$. $E_c=0.8$. Upper panel: Magnetization m in a FM state for $U/t=24$ and $T/t=0.1$. Lower panel: In-plane staggered magnetization m_{stagg} in an AF state for $U/t=6$ and $T/t=0.05$. Filled (open) circles are the results by DMFT (HF). For comparison, charge density n_{tot} computed by DMFT is also shown in the lower panel (filled squares). Note that the staggered magnetization in the outer layers ($|z| \geq 2$), and the outermost layers ($|z|=1$) have the same sign.

with E_c . This indicates that the FM ordering is favored by the intermediate charge densities as discussed in the bulk single-band Hubbard model;²² at large E_c , the magnetization is large on the outer layer and small in the inner layer; at small E_c , the situation is reversed.

These arguments are confirmed by our calculations of the spatial variation of the magnetization density, reported in Fig. 2, which shows numerical results for a four-layer heterostructure with counterions at $z=\pm 0.5$ and ± 1.5 , and $E_c=0.8$. The upper panel of Fig. 2 shows the magnetization in the FM state. In DMFT (filled circles), only the layers near the interfaces ($|z| \sim 1-2$) have large polarization and inner layers in the heterostructure have small moments. This explains the weak n dependence of T_C of thick heterostructures (see the upper panel of Fig. 1). In HF (open circles), all layers in the heterostructure are highly polarized. In contrast in an AF state, result of the in-plane staggered magnetization by DMFT and HF agree well as shown in the lower panel of Fig. 2. For comparison, the total charge density is also plotted (filled squares). The in-plane staggered magnetization is large only at inner layers where the charge density is close to 1. Note that the staggered magnetization in the outer layers ($|z| \geq 2$) has the same sign as in the edge layers ($|z|=1$) indicating that the outer layers are not intrinsically magnetic.

We now return to the issue of fluctuation effects. We study a model which is two-dimensional and order parameters with a continuous spin rotation symmetry; thus, at $T > 0$, rather the calculated T_C means a crossover to a low- T “almost or-

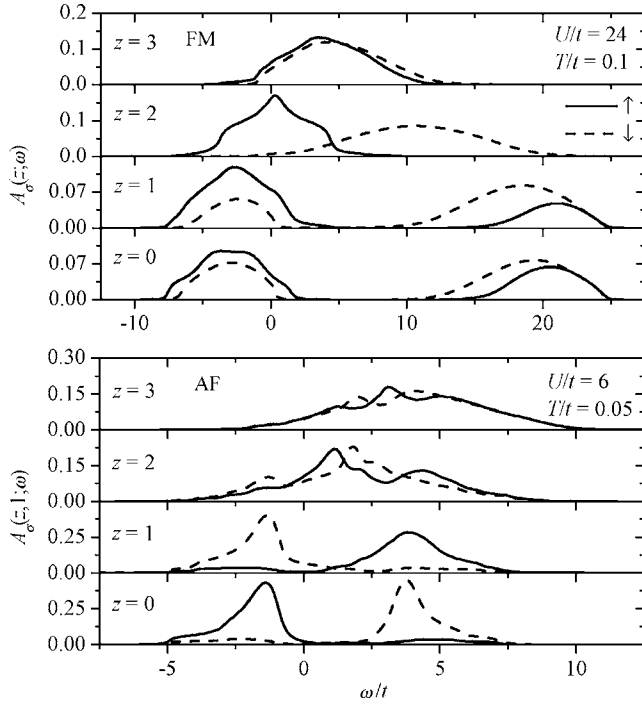


FIG. 3. Layer- and sublattice-resolved spectral functions as functions of real frequency ω for four-layer heterostructure. $E_c=0.8$. Upper panel: Ferromagnetic state at $U/t=24$ and $T/t=0.1$. Lower panel: Antiferromagnetic state at $U/t=6$ and $T/t=0.05$. Sublattice $\eta=1$. Solid (broken) lines are for up (down) spin electrons. For sublattice $\eta=2$ in AF state, up and down electrons are interchanged.

dered" phase characterized by an exponentially growing correlation length $\xi \sim \exp(2\pi\rho_s/T)$ ¹⁹ where the key stiffness ρ_s is given by the second derivative of the free energy with respect to the order parameter orientation. We have computed ρ_s for a single ferromagnetic plane with charge density 0.5 finding $\rho_s \sim t/8$. We observe that in all cases several planes exhibit the relevant order, so that the total stiffness is larger by a factor 2–3. Thus we see that the stiffness is large enough relative to the DMFT $T_{C,N}$'s that the purely two-dimensional fluctuation effects are of minor importance, leading to $\xi > \exp(4-5)$ for $T < T_{C,N}/2$.

The spin distributions presented in Fig. 2 can be understood from the single-particle spectral functions. In Fig. 3 are presented the DMFT results for the layer- and sublattice-resolved spectral functions $A_\sigma(z, \eta; \omega) = -1/\pi \text{Im} G_\sigma^{\text{imp}}(z, \eta; \omega + i0^+)$ for the FM (upper panel) and the AF (lower panel) states of four-layer heterostructure with the same parameters as in Fig. 2. These quantities can in principle be measured by spin-dependent photoemission or scanning tunneling microscopy. As noticed in Ref. 18, the spectral function outside of the heterostructure ($|z| \gg 2$) is essentially identical to that of the free tight-binding model H_{bands} and electron density is negligibly small. With approaching the interfaces ($|z|=2$), the spectral function shifts

downwards and begins to broaden. In the FM case, magnetic ordering is possible only near the interface layers ($|z| \sim 1-2$) carrying the intermediate charge density. Inside the heterostructure ($|z| \ll 2$), clear Hubbard gap exists due to the large U and uniform polarization is hard to achieve. On the contrary, high charge density is necessary to keep the staggered magnetization in the AF case as seen as a difference between up and down spectra in the lower panel of Fig. 3.

So far, we have discussed the competition between ferromagnetic and antiferromagnetic phases and spatial distributions of charge and magnetic densities establishing that ferromagnetism is a surface effect. Finally, we discuss the interplay between phases. We note that the charge density or magnetization density typically varies over ~ 3 unit cell range, so for thin heterostructures and moderate charge confinement energies, the entire heterostructure exhibits a single phase, controlled by the instability exhibiting the highest transition temperature (cf. Fig. 1). However, for thicker heterostructure or stronger confinement we believe that one can observe an ordered state involving an antiferromagnetic center with a ferrimagnetic "skin." A hint of this behavior can be observed in Fig. 2. Consider the central layer; this has an occupancy $n_{\text{tot}} \approx 0.9$, so from Fig. 1 and rescaling account for the different U , we would expect $T_N \sim 0.1t$. Now this layer is not isolated; hopping to the layers at $z = \pm 1$ leads to an effective polarizing field of the order of $2(1-n_{\text{tot}})tm/n_{\text{tot}}$ where the first factor is the number of layers, the second is the hopping amplitude renormalized by strong correlations, and the third factor is the relative spin polarization; putting these factors together gives a polarizing field of about $0.15t$, approximately equal to the AF coupling. Thus for the central layer of this heterostructure ferromagnetic and antiferromagnetic tendencies are very closely balanced, but for thicker systems (not at present computationally accessible) or perhaps for stronger charge confinement, an antiferromagnetic center surrounded by a FM skin is likely to occur.

To summarize, we have presented a semiclassical DMFT study of magnetic phase behavior of a model Mott-insulator-band-insulator heterostructure in which the behavior is controlled by the spreading of the electronic charge out of the confinement region. The magnetic phase diagram is investigated as a function of layer thickness, temperature, and interaction strength. Ferromagnetic ordering is found to be a surface effect stabilized at an interface region with moderate charge density, while antiferromagnetic ordering is found at a region with high density ~ 1 characteristic of the bulk Mott insulator, and Néel temperature is sensitive to the layer thickness and charge confinement energy. We suggest that these magnetic orderings may coexist in very thick heterostructure exhibiting a ferromagnetic skin and an antiferromagnetic "core."

We acknowledge fruitful discussions with G. Kotliar, P. Sun, J. Chakhalian, D. Vollhardt, and Th. Pruschke. This research was supported by JSPS (S.O.) and the DOE under Grant No. ER 46169 (A.J.M.).

*Electronic address: okapon@phys.columbia.edu

- ¹M. Imada, A. Fujimori, and Y. Tokura, *Rev. Mod. Phys.* **70**, 1039 (1998).
- ²Y. Tokura and N. Nagaosa, *Science* **288**, 462 (2000).
- ³C. H. Ahn, S. Gariglio, P. Paruch, T. Tybell, L. Antognazza, and J.-M. Triscone, *Science* **284**, 1152 (1999).
- ⁴S. Gariglio, C. H. Ahn, D. Matthey, and J.-M. Triscone, *Phys. Rev. Lett.* **88**, 067002 (2002).
- ⁵A. Ohtomo, D. A. Muller, J. L. Grazul, and H. Y. Hwang, *Nature (London)* **419**, 378 (2002).
- ⁶M. Izumi, Y. Ogimoto, Y. Konishi, T. Manako, M. Kawasaki, and Y. Tokura, *Mater. Sci. Eng., B* **84**, 53 (2001), and references therein.
- ⁷A. Biswas, M. Rajeswari, R. C. Srivastava, Y. H. Li, T. Venkatesan, R. L. Greene, and A. J. Millis, *Phys. Rev. B* **61**, 9665 (2000).
- ⁸A. Biswas, M. Rajeswari, R. C. Srivastava, T. Venkatesan, R. L. Greene, Q. Lu, A. L. deLozanne, and A. J. Millis, *Phys. Rev. B* **63**, 184424 (2001).
- ⁹M. Potthoff and W. Nolting, *Phys. Rev. B* **60**, 7834 (1999).
- ¹⁰S. Schwieger, M. Potthoff, and W. Nolting, *Phys. Rev. B* **67**, 165408 (2003).
- ¹¹A. Liebsch, *Phys. Rev. Lett.* **90**, 096401 (2003).
- ¹²R. Matzdorf, Z. Fang, Ismail, J. Zhang, T. Kimura, Y. Tokura, K. Terakura, and E. W. Plummer, *Science* **289**, 746 (2000).
- ¹³M. Potthoff and W. Nolting, *Phys. Rev. B* **52**, 15341 (1995).
- ¹⁴Z. Fang, I. V. Solovyev, and K. Terakura, *Phys. Rev. Lett.* **84**, 3169 (2000).
- ¹⁵S. Okamoto, A. Fuhrmann, A. Comanac, and A. J. Millis, *Phys. Rev. B* **71**, 235113 (2005).
- ¹⁶A. Georges, B. G. Kotliar, W. Krauth, and M. J. Rozenberg, *Rev. Mod. Phys.* **68**, 13 (1996).
- ¹⁷S. Okamoto and A. J. Millis, *Nature (London)* **428**, 630 (2004); *Phys. Rev. B* **70**, 075101 (2004).
- ¹⁸S. Okamoto and A. J. Millis, *Phys. Rev. B* **70**, 241104(R) (2004).
- ¹⁹S. Sachdev, *Quantum Phase Transitions* (Cambridge University Press, Cambridge, 1999).
- ²⁰M. Potthoff, *Phys. Rev. B* **64**, 165114 (2001).
- ²¹R. Zitzler, T. Pruschke, and R. Bulla, *Eur. Phys. J. B* **27**, 473 (2002).
- ²²P. J. H. Denteneer and M. Blaauboer, *J. Phys.: Condens. Matter* **7**, 151 (1995).